Article

Influence of Stereochemistry and Redox Potentials on the Single- and Double-Strand DNA Cleavage Efficiency of Cu(II)· and Ni(II)·Lys-Gly-His-Derived ATCUN Metallopeptides

Yan Jin, Mark A. Lewis, Nikhil H. Gokhale, Eric C. Long, and J. A. Cowan

J. Am. Chem. Soc., **2007**, 129 (26), 8353-8361• DOI: 10.1021/ja0705083 • Publication Date (Web): 07 June 2007

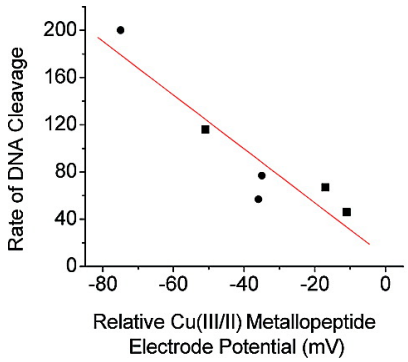

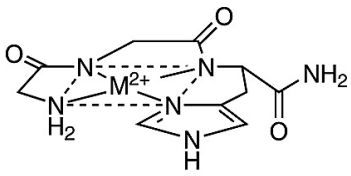

More About This Article

Additional resources and features associated with this article are available within the HTML version:

- Supporting Information
- Links to the 4 articles that cite this article, as of the time of this article download
- Access to high resolution figures
- Links to articles and content related to this article
- Copyright permission to reproduce figures and/or text from this article

View the Full Text HTML

J|A|C|S
ARTICLES
Published on Web 06/07/2007

Influence of Stereochemistry and Redox Potentials on the Single- and Double-Strand DNA Cleavage Efficiency of Cu(II)· and Ni(II)·Lys-Gly-His-Derived ATCUN Metallopeptides

Yan Jin,[†] Mark A. Lewis,[‡] Nikhil H. Gokhale,[†] Eric C. Long,*[,‡] and J. A. Cowan*[,†]

Contribution from the Evans Laboratory of Chemistry, The Ohio State University, 100 West 18th Avenue, Columbus, Ohio 43210, and the Department of Chemistry & Chemical Biology, Purdue School of Science, Indiana University-Purdue University Indianapolis, 402 North Blackford Street, Indianapolis, Indiana 46202

Received January 25, 2007; E-mail: cowan@chemistry.ohio-state.edu; long@chem.iupui.edu

Abstract: The DNA cleavage chemistry of a series of metallopeptides based on the amino-terminal Cu and Ni (ATCUN) binding motif of proteins has been studied. Specifically, the impact of the positioning of charged Lys side chains and their stereochemistry on metal reduction potentials and DNA cleavage reactivity have been quantitatively evaluated. Both Cu and Ni metallopeptides show a general increase in reactivity toward DNA with an increasing number of Lys residues, while a corresponding decrease in complex reduction potential reflects the enhanced σ-donor character of the Lys side chain relative to that of Gly. Placement of Lys at the first position in the tripeptide ligand sequence resulted in a greater increase in DNA cleavage reactivity, relative to placement at the second position, while a switch from an L-Lys to a D-Lys typically resulted in enhanced reactivity, as well as perturbations of reduction potential. In the case of Cu peptides, reactivity was enhanced with both increasing positive charge density on the peptide and stabilization of the Cu^{3+} state. However, for Ni peptides, while the general trends are the same, the correlation with redox behavior was less pronounced. Most likely these differences in specific trends for the Cu and Ni complexes reflect the distinct coordination preferences for $Cu^{3+/2+}$ and $Ni^{3+/2+}$ oxidation states, and the consequent distinct positioning of metal-associated reactive oxygen species, as well as the orientation of the DNA-associated complex. Thus, the amino acid composition and stereochemistry of ATCUN metallopeptides can tune the intrinsic reactivities of these systems (their ability to promote formation and activity of metal-associated ROS) as well as their overall structural features, and both of these aspects appear to influence their reactivity and efficiency of DNA strand scission.

Introduction

Metallopeptides of the general form M(II)·Gly-Gly-His (Scheme 1) represent minimalist versions of the amino-terminal Cu^{2+} and Ni^{2+} (ATCUN)[1] binding motif of proteins and peptides. ATCUN motifs, for example, occur naturally in the albumins,[1] histatins,[2] and the human DNA binding protein protamine P2.[3] Along with the occurrence of this sequence in native proteins, the low molecular weight metallotripeptide Cu(II)·Gly-Gly-His is active against Ehrlich ascites tumor cells[4] and has been shown to induce DNA cleavage when activated with ascorbate;[5] this system also effects DNA strand scission as a synthetic[6] or biosynthetic[7] appendage to DNA binding proteins. In addition to DNA cleavage by ascorbate-activated Cu^{2+} derivatives of this motif, which appear to cleave DNA through the production of nondiffusible, reduced oxygen species,[6] Ni(II)·Gly-Gly-His can also induce DNA or RNA scission

Scheme 1. Structure of M(II)·Gly-Gly-His

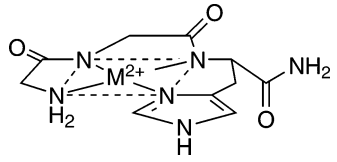

[†] The Ohio State University.
[‡] Indiana University-Purdue University Indianapolis.

(1) (a) Harford, K.; Sarkar, B. *Acc. Chem. Res.* **1997**, *30*, 123−130. (b) Camerman, N.; Camerman, A.; Sarkar, B. *Can. J. Chem.* **1976**, *54*, 1309−1316.
(2) (a) Gusman, H.; Lendenmann, U.; Grogan, J.; Troxler, R. F.; Oppenheim, F. G. *Biochim. Biophys. Acta* **2001**, *1545*, 86−95. (b) Melino, S.; Gallo, M.; Trotta, E.; Mondello, F.; Paci, M.; Petruzzelli, R. *Biochemistry* **2006**, *45*, 15373−15383.
(3) (a) Bal, W.; Wojcik, J.; Maciejczyk, M.; Grochowski, P.; Kasprzak, K. S. *Chem. Res. Toxicol.* **2000**, *13*, 823−830. (b) Bal, W.; Jezowska-Bojczuk, M.; Kasprazak, K. S. *Chem. Res. Toxicol.* **1997**, *10*, 906−914. (c) Bal, W.; Lukszo, J.; Kasprzak, K. S. *Chem. Res. Toxicol.* **1997**, *10*, 915−921. (d) McKay, D. J.; Renaux, B. S.; Dixon, G. H. *Eur. J. Biochem.* **1986**, *156*, 5−8.
(4) Kimoto, E.; Tanaka, H.; Gyotoku, J.; Morishige, F.; Pauling, L. *Cancer Res.* **1983**, *43*, 824−828.
(5) Chiou, S.-H. *J. Biochem.* **1983**, *94*, 1259−1267.
(6) (a) Mack, D. P.; Dervan, P. B. *Biochemistry* **1992**, *31*, 9399−9405. (b) Mack, D. P.; Dervan, P. B. *J. Am. Chem. Soc.* **1990**, *112*, 4604−4606. (c) Mack, D. P.; Iverson, B. L.; Dervan, P. B. *J. Am. Chem. Soc.* **1988**, *110*, 7572−7574.
(7) (a) Nagaoka, M.; Hagihara, M.; Kuwahara, J.; Sugiura, Y. *J. Am. Chem. Soc.* **1994**, *116*, 4085−4086. (b) Harford, C.; Narindrasorasak, S.; Sarkar, B. *Biochemistry* **1996**, *35*, 4271−4278.

when activated similarly or through peroxide-based reagents.[8] Given their ability to oxidatively modify substrates, Gly-Gly-His metallotripeptides have been exploited in the generation of low molecular weight peptide,[9] drug,[10] oligonucleotide-,[11] or PNA-based[12] conjugates, protein scission and cross-linking reagents,[13] and as agents to understand Ni-based toxicity.[3,14] In addition, these agents have been used to probe fundamental peptide and amino acid interactions with DNA or RNA.[8] Notably, recent results from one of our laboratories[15] have revealed the high level of DNA cleavage efficiency that can be achieved with Cu(II)·Gly-Gly-His-derived metallopeptides in comparison to other systems. Of particular interest, Cu(II)·Gly-Gly-His-derived metallopeptides have been found to induce the linearization of DNA to an extent greater than expected through a simple accumulation of single-strand cleavage events.[15]

Promoting their study and application, Cu^{2+} and Ni^{2+} bind to Gly-Gly-His and to Xaa-Xaa-His tripeptides in general, with high affinity through coordination to the terminal peptide amine, two intervening deprotonated peptide amides, and the His imidazole (Scheme 1).[1,16] These systems are well-characterized, exist as 1:1 transition-metal complexes at physiological pH, and have served to model the Ni^{2+} and Cu^{2+} transport domains of the serum albumins.[1,17] Given that metal binding within the tripeptide ligand occurs through main-chain atoms of the first two amino acid residues without direct side-chain involvement, Gly can be substituted for any α-amino acid in these two positions; however, it has been demonstrated that certain amino acid substitutions lead to further stabilization of the metal-bound species.[16] Overall, these metal-bound systems are quite stable under physiological conditions, making them possible candidates for in vivo applications or peptidomimetic development.

As nucleic acid cleavage agents, M(II)·Gly-Gly-His metallopeptides are unique in their ability to position at the periphery of a metal complex framework the same chemical functional groups used by proteins and peptide-based natural product antitumor agents for DNA and RNA molecular recognition.[18] Thus, one of our laboratories has exploited the well-defined environment of Ni(II)·Gly-Gly-His-derived metallopeptides and the ability to control the orientation of side-chain functional groups in synthetic peptides through choice of the stereochemistry at select α-carbon centers to increase our knowledge of peptide−nucleic acid recognition events.[8] Indeed, it has been determined that Ni(II)·Gly-Gly-His-derived metallopeptides, when activated with peroxides, cleave DNA site-selectively[19] as a function of their amino acid composition and stereochemistry via a minor groove interaction and C4′−H abstraction.[20] Amino acid side-chain composition and stereochemistry influence the overall efficiency of DNA strand scission by Ni(II)·Gly-Gly-His-derived metallopeptides as well.[19,21]

Recently, details of the minor groove recognition of these metallopeptide systems have been revealed through experimental[21−23] and theoretical[21,22,24] means. It appears likely that, during the course of their interactions with DNA, Ni(II)·Arg-Gly-His and similar metallopeptides insert their imidazole/N-terminal, square-planar "edges" into the minor groove to form transient H bonds from the imidazole pyrrole N−H, N-terminal N−H protons, and Arg side chain to H-bond acceptors on the floor of the minor groove of A/T-rich regions (i.e., via the O2 of T and the N3 of A). Further recent studies have sought to explain the influence of amino acid stereochemistry on the DNA cleavage site selectivity exhibited by Ni(II)·L/D-Arg/Lys-Gly-His systems.[21,22] We have reported that an L-Arg residue in the amino-terminal peptide position can align along the minor groove to produce an isohelical metallopeptide that facilitates interaction with the DNA at select A/T-rich locations. In comparison, a D-Arg residue in this same position creates a metallopeptide diastereoisomer that is sterically less compatible with the DNA minor groove, consequently leading to less selective, but more frequent and efficient DNA cleavage within a given A/T-rich DNA site. In contrast, stereochemical substitutions within the middle peptide position (e.g., as in Ni(II)·Gly-L/D-Lys-His) do not influence site selectivity beyond what is observed with a Gly substitution; however, increased DNA cleavage efficiency is observed in the case of D-residues.[21] Thus, metallopeptide diastereoisomers result in unique DNA cleavage site-selectivities and varied levels of cleavage efficiency.

Herein, we describe studies aimed at defining additional factors that influence the DNA cleavage efficiency of M(II)·Gly-Gly-His systems. These studies include an investigation into the influences of amino acid α-carbon stereochemistry, the positioning and number of positive charges within the metallopeptide framework, and intrinsic redox properties on DNA cleavage mediated by both Cu(II)· and Ni(II)·Gly-Gly-His-derived metallopeptides. These investigations were carried out through kinetic analyses and electrochemical investigations. The information gained could likely influence the rational design of efficient DNA minor groove-directed cleavage[8,15d] agents that may function under physiological conditions.

(8) (a) Long, E. C.; Claussen, C. A. In *DNA and RNA Binders: From Small Molecules to Drugs*; Demeunynk, M., Bailly, C., Wilson, W. D., Eds.; Wiley-VCH: New York, 2003; pp 88−125. (b) Long, E. C. *Acc. Chem. Res*. **1999**, *99*, 827−836.
(9) Shullenberger, D. F.; Long, E. C. *Bioorg. Med. Chem. Lett*. **1993**, *3*, 333−336.
(10) (a) Grokhovsky, S. L.; Nikolaev, V. A.; Zubarev, V. E.; Surovaya, A. N.; Zhuze, A. L.; Chernov, B. K.; Sidorova, N.; Zasedatelev, A. S. *Mol. Biol. (Moscow, Russ. Fed., Engl. Ed.)* **1992**, *26*, 1274−1297. (b) Morier-Teissier, E.; Boitte, N.; Helbecque, N.; Bernier, J. L.; Pommery, N.; Duvalet, J. L.; Fournier, C.; Hecquet, B.; Catteau, J. P.; Henichart, J. P. *J. Med. Chem.* **1993**, *36*, 2084−2090. (c) Steullet, V.; Dixon, D. W. *Bioorg. Med. Chem. Lett.* **1999**, *9*, 2935−2940.
(11) (a) De Napoli, L.; Messere, A.; Montesarchio, D.; Piccialli, G.; Benedetti, E.; Bucci, E.; Rossi, F. *Bioorg. Med. Chem. Lett.* **1999**, *7*, 395−400. (b) Truffert, J.-C.; Asseline, U.; Brack, A.; Thuong, N. T. *Tetrahedron* **1996**, *52*, 3005−3016.
(12) Footer, M.; Egholm, M.; Kron, S.; Coull, J. M.; Matsudaira, P. *Biochemistry* **1996**, *35*, 10673−10679.
(13) Van Dijk, J.; Lafont, C.; Knetsch, M. L. W.; Derancourt, J.; Manstein, D. J.; Long, E. C.; Chaussepied, P. *J. Muscle Res. Cell Motil*. **2004**, *25*, 527−537.
(14) Muller, J. G.; Hickerson, R. P.; Perez, R. J.; Burrows, C. J. *J. Am. Chem. Soc.* **1997**, *119*, 1501−1506.
(15) (a) Jin, Y.; Cowan, J. A. *J. Am. Chem. Soc.* **2005**, *127*, 8408−8415. (b) Jin, Y.; Cowan, J. A. *J. Am. Chem. Soc.* **2006**, *128*, 410−411. (c) Sreedhara, A.; Freed, J. D.; Cowan, J. A. *J. Am. Chem. Soc.* **2000**, *122*, 8814−8824. (d) Cowan, J. A. *Curr. Opin. Chem. Biol.* **2001**, *5*, 634−642.
(16) Kozlowski, H.; Bal, W.; Dyba, M.; Kowalik-Jankowska, T. *Coord. Chem. Rev*. **1999**, *184*, 319−346.
(17) Lau, S.-J.; Kruck, T. P. A.; Sarkar, B. *J. Biol. Chem.* **1974**, *249*, 5878−5884.
(18) (a) Steitz, T. A. *Q. Rev. Biophys.* **1990**, *23*, 205−280. (b) Zimmer, C.; Wahnert, U. *Prog. Biophys. Mol. Biol.* **1986**, *47*, 31−112.
(19) Liang, Q.; Eason, P. D.; Long, E. C. *J. Am. Chem. Soc.* **1995**, *117*, 9625−9631.
(20) Liang, Q.; Ananias, D. C.; Long, E. C. *J. Am. Chem. Soc*. **1998**, *120*, 248−257.
(21) Fang, Y.-Y.; Claussen, C. A.; Lipkowitz, K. B.; Long, E. C. *J. Am. Chem. Soc.* **2006**, *128*, 3198−3207.
(22) Fang, Y.-Y.; Ray, B. D.; Claussen, C. A.; Lipkowitz, K. B.; Long, E. C. *J. Am. Chem. Soc.* **2004**, *126*, 5403−5412.
(23) Nagane, R.; Koshigoe, T.; Chikira, M.; Long, E. C. *J. Inorg. Biochem.* **2001**, *83*, 17−23.
(24) Fang, Y.-Y.; Lipkowitz, K. B.; Long, E. C. *J. Chem. Theory Comput*. **2006**, *2*, 1453−1463.

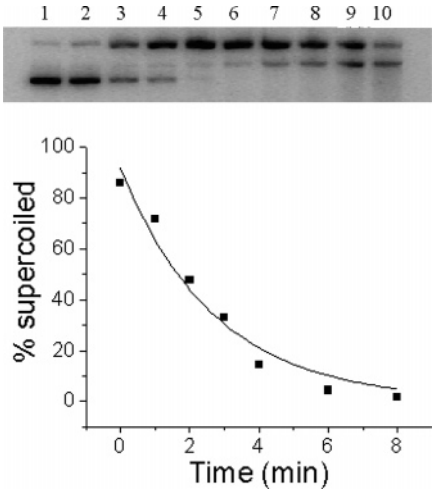

Figure 1. Time course of the DNA cleavage activity of Cu(II)·Lys-Gly-His-Lys. Gel image (top) showing the formation of nicked (upper band) and linear (middle band) DNA products from a supercoiled (lower band) substrate DNA as monitored by 0.8% agarose gel electrophoresis. All lanes contained 50 μM DNA (base pair concentration), 40 μM Cu(II)·Lys-Gly-His-Lys, and 400 μM ascorbate in 20 mM Tris buffer, pH 7.4, 37 °C; lanes 1−10: 0, 1, 2, 3, 4, 6, 8, 10, 12, and 15 min reaction times prior to quenching with EDTA-containing buffer, respectively. The reaction curve (bottom) derived from data obtained from lanes 1−7 exhibits a pseudo-first-order kinetic profile ($R^2 = 0.97$), $k_{obs} \approx 0.37$ min^{-1}.

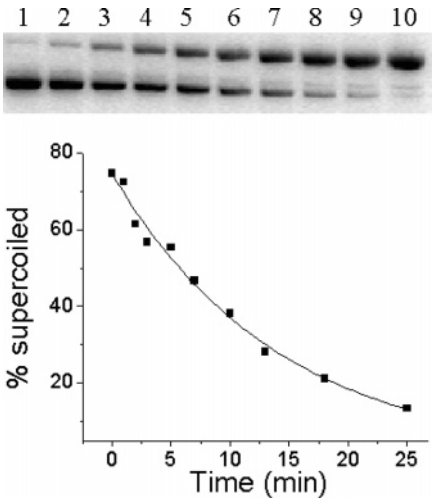

Figure 2. Time course of the DNA cleavage activity of Ni(II)·Lys-Gly-His. Gel image (top) showing the formation of nicked (upper band) and linear (middle band) DNA products from a supercoiled (lower band) DNA substrate as monitored by 0.8% agarose gel electrophoresis. All lanes contained 50 μM DNA (base pair concentration), 5 μM Ni(II)·Lys-Gly-His, and 200 μM $KHSO_5$ in 20 mM sodium cacodylate buffer, pH 7.4, 37 °C; lanes 1−10: 0, 1, 2, 3, 5, 7, 10, 13, 18, and 25 min reaction times prior to quenching with EDTA-containing buffer, respectively. The reaction curve (bottom) indicates a pseudo-first-order kinetic profile ($R^2 = 0.99$), $k_{obs} \approx 0.07$ min^{-1}.

Experimental Section

General Materials and Methods. All peptides employed in this study were synthesized through standard manual Fmoc solid-phase synthesis protocols using commercially available protected amino acids and Rink-amide resins (Bachem). Upon final deprotection, these procedures yielded peptides with carboxamide termini. All amino acids used were of the L-configuration unless specified otherwise. Peptide purities and identities were confirmed using LC−MS and MALDI-TOF mass spectroscopy. All data shown are the average of at least triplicate experiments. Unless stated otherwise, all reagents used in this research were obtained from Sigma Chemical Co.

Metallopeptide Synthesis and Characterization. Solutions of 1 mM ATCUN peptide in 20 mM Tris buffer (pH 7.4) were mixed with 0.8 mM $CuCl_2$ or 0.8 mM $NiSO_4$ in 20 mM Tris buffer, pH 7.4 (or 20 mM sodium cacodylate buffer, pH 7.4) in 1:1 v/v ratios. These mixtures yielded solutions containing up to 1.25:1 peptide/metal ratios, effectively eliminating free Cu^{2+} or Ni^{2+} ion in DNA cleavage reaction mixtures. The resulting solutions were stirred at room temperature for ∼30 min, resulting in light reddish-purple solutions for Cu^{2+}−peptide complexes and yellow solutions for Ni^{2+}−peptide complexes; these systems displayed UV−vis spectra as observed previously.[1] Samples were maintained at 4 °C, and concentrations and stabilities of the metallopeptide complexes were routinely verified prior to use.

DNA Cleavage Studies. Plasmid pUC19 (2686 base pairs) was purchased from New England Biolabs, Inc. The plasmid was transformed into DH5α competent cells, amplified,[15c] and subsequently isolated and purified using QIAGEN protocols. Fresh plasmid DNA (more than 90−95% supercoiled) was prepared before each experiment to avoid contamination by any other form of plasmid DNA. In general, DNA cleavage experiments were performed by prompt mixing of 50 μM base pair concentration of pUC19, 20 μM M(II)−peptide, and 200 μM ascorbate (or $KHSO_5$) in 20 mM Tris buffer, pH 7.4 (or 20 mM sodium cacodylate buffer, pH 7.4), at 37 °C. The concentration of metallopeptide catalyst used in a specific experiment typically varied from 4 to 40 μM, with experiments employing oxone ($KHSO_5$) requiring a lower catalyst concentration to achieve an optimal time frame for evaluation of kinetic rate constants. Control reactions were carried out in parallel using the same conditions as the cleavage reactions, but lacked the M(II)·peptide complex. All reactions were quenched with a loading buffer containing 0.5 M EDTA.[25] Analyses were performed via standard agarose gel electrophoresis using gels (0.8%) that contained ethidium bromide.[25] DNA samples were run on horizontal gels in 1× TAE buffer for 90 min at 120 mV.

DNA Cleavage Quantitation. Quantitation of closed circular (supercoiled), nicked, and linear DNA was made by densitometric analysis of ethidium bromide containing agarose gels. Quantitation was performed by fluorescence imaging using a Gel-Doc 1000 (BioRad) and data analysis with Multianalysis software (version 1.1) provided by the manufacturer using the volume quantitation method. In all cases, background fluorescence was subtracted by reference to a lane containing no DNA. A correction factor of 1.47 was used for supercoiled DNA, since the ability of ethidium bromide to intercalate into supercoiled DNA (Form I) is decreased relative to nicked (Form II) and linear DNA (Form III). The fraction of each form of DNA was calculated by dividing the intensity of each band by the total intensities of all the bands in the lane. All results were obtained from experiments that were performed at least in triplicate.

Influence of NaCl on DNA Cleavage. The ionic strength dependence of metallopeptide−DNA cleavage activity was evaluated over a range of NaCl concentrations (0, 4, 40, 150, and 400 mM). In general, DNA cleavage experiments by Cu(II)−peptide complexes were performed with 50 μM base pair concentrations of pUC19 plasmid DNA, 40 μM complex, and 500 μM ascorbate in 20 mM Tris buffer, pH 7.4 at 37 °C. In the case of Ni(II)−peptide complexes, DNA cleavage reactions were carried out with 50 μM base pair concentrations of pUC19 plasmid DNA, 4 μM complex, and 50 μM $KHSO_5$ in 20 mM sodium cacodylate buffer, pH 7.4 at 37 °C. Control reactions were carried out using the same conditions as the cleavage reactions, but lacking a M(II)−peptide complex. All reactions were quenched with a loading buffer containing 0.5 M EDTA. Agarose gel electrophoresis (0.8%) containing ethidium bromide was performed under standard conditions. DNA samples were run on horizontal gels in 1× TAE buffer for 90 min at 120 mV.

Analysis of DNA Linearization. Following DNA cleavage, the fraction of full length, linear DNA (Form III) was related to the number,

(25) Sambrook, J.; Fritsch, E. F.; Maniatis, T. *Molecular Cloning*; Cold Spring Harbor Laboratory Press: New York, 1989.

$n2$, of double-strand breaks per molecule given by the first term of a Poisson distribution (eq 1).[26]

$$f(\mathrm{III}) = n2 \exp(-n2) \quad (1)$$

The sum of single-strand, $n1$, and double-strand, $n2$, breaks per molecule ($n1 + n2$) was determined from the fraction of Form I, supercoiled DNA remaining after treatment with the metallopeptide.[26]

$$f(\mathrm{I}) = \exp[-(n1 + n2)] \quad (2)$$

The Freifelder−Trumbo relation (eq 2) shows that the number of double-strand breaks expected from coincidences of random single-strand breaks is less than 0.01 per molecule, ($n1/n2$) > 100.[27] Consequently, from comparison of the ratio of $n1$ and $n2$ ($n1/n2$) relative to 100, one can determine if the linearization of DNA resulted from random or nonrandom cleavage. In these studies, both $n1$ and $n2$ were calculated using eqs 1 and 2.

Determination of Electrode Potentials for Cu(II)· and Ni(II)·ATCUN Complexes. Cyclic voltammetry (CV) and square-wave voltammetry (SWV) data were collected with a Princeton Applied Research model PAR 263 potentiostat/galvanostat. The instrument was controlled with Princeton Applied Research Headstart (V1.5) software with a GPIB interface. A glassy carbon working electrode (3-mm diameter), platinum wire auxiliary electrode, and Vycor tip Ag/AgCl reference electrode stored in 3 M NaCl ($E° = 0.197$ V vs NHE) were used. The glassy carbon electrode was polished (using polishing alumina followed by 1-μm diamond polish obtained from BAS) before each experiment. The analyte solutions were made in 25 mM phosphate buffer (pH 7.4) containing 0.1 M KCl, 1 mM Cu(II)−peptide or Ni(II)−peptide (metal/peptide ratio 1:1.1) and were argon-purged prior to each measurement.

Results

DNA Cleavage Reactivity of Cu(II)· and Ni(II)·ATCUN Metallopeptides. The DNA cleavage activities of two typical M(II)·ATCUN complexes containing Cu and Ni are shown in Figures 1 and 2, respectively. Consistent with prior studies,[15a] DNA cleavage activity was observed to be dependent upon catalyst concentration but exhibited no saturation behavior reminiscent of an enzyme; the rates of DNA cleavage correspond to a second-order reaction. Consequently, all reactions were considered in terms of the standard rate law shown in eq 3 with the initial rate (V_0), corresponding to less than 5% substrate conversion, considered as a function of [metallopeptide] as shown in eqs 4 and 5.

$$\mathrm{Rate} = V_t = \mathrm{d[DNA]}_t/\mathrm{d}t = k_2[\mathrm{DNA}]_t^m[\mathrm{metallopeptide}]_t, \quad (\text{where } m = 1) \quad (3)$$

when

$$t = 0,\ V_0 = k_2[\mathrm{DNA}]_0^m[\mathrm{metallopeptide}]_0 \quad (4)$$

and

$$\ln V_0 = m \ln[\mathrm{DNA}]_0 + \ln(k_2[\mathrm{metallopeptide}]_0) \quad (5)$$

As reported earlier for Cu(II)·ATCUN metallopeptides,[15a] a plot of ln V_0 versus ln[DNA]$_0$ at constant [Ni(II)·Lys-Gly-His]$^+$ concentration (Figure 3) yielded a value of $m \approx 1$ for DNA, again consistent with a reaction that is first-order in DNA concentration, as shown in Figures 1 and 2. Similarly, second-order reaction rate constants k_2 were systematically determined for a variety of Cu^{2+} or Ni^{2+} metallopeptides (Tables 1 and 2). Overall, the Cu(II)−peptide complexes were found to be more efficient DNA cleavage agents than the corresponding Ni(II)−peptide complexes when ascorbate was employed as a co-reactant (Table 1); however, with $KHSO_5$ as a co-reactant in sodium cacodylate buffer, reactivities of the Ni(II)−peptide complexes were found to increase significantly (Table 2). Although the activity of Cu(II)−peptide complexes also increased under the same reaction conditions, the extent of improvement was smaller than that found for the Ni(II)−peptide complexes (Table 2). The reactivity of the Cu and Ni complexes was relatively insensitive to the buffer system used.

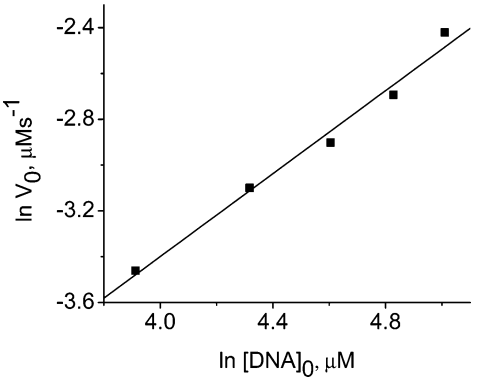

Figure 3. Rate law studied in 20 mM sodium cacodylate buffer, pH 7.4, 37 °C, where [Ni(II)·Lys-Gly-His] = 10 μM, [$KHSO_5$] = 200 μM. The dependence of ln V_0 versus ln[DNA]$_0$ was fitted, where $k_{obs} = k_2$[complex], and yielded $k_2 \approx 106$ M^{-1} s^{-1} and $m \approx 1$ ($R^2 = 0.99$).

Table 1. Rates of DNA Cleavage Observed for Cu(II)· and Ni(II)·ATCUN Metallopeptides Activated with Ascorbate[a]

peptide–ligand	Cu(II)·ATCUN (k_2, M^{-1} s^{-1})	Ni(II)·ATCUN (k_2, M^{-1} s^{-1})
Gly-Gly-His	36 ± 2	13 ± 1
Gly-Lys-His	46 ± 3	19 ± 1
Gly-D-Lys-His	57 ± 4	23 ± 1
Lys-Gly-His	67 ± 4	21 ± 1
D-Lys-Gly-His	77 ± 4	26 ± 1
Lys-Gly-His-Lys	109 ± 4	34 ± 4
Lys-Lys-His	116 ± 7	35 ± 2
D-Lys-D-Lys-His	200 ± 11	34 ± 1

[a] All peptides contain C-terminal amides. Data were obtained in 20 mM Tris buffer, pH 7.4, with 200 μM ascorbate as co-reactant. Amino acids are L-configuration unless noted.

Table 2. Rates of DNA Cleavage Observed for Various Lys-Containing ATCUN Metallopeptides Activated with $KHSO_5$[a]

complex	k_2 (M^{-1} s^{-1})
Cu(II)·Lys-Gly-His	162 ± 15
Ni(II)·Lys-Gly-His	106 ± 11
Cu(II)·D-Lys-D-Lys-His	283 ± 22
Ni(II)·D-Lys-D-Lys-His	255 ± 25

[a] Data were obtained in 20 mM sodium cacodylate buffer, pH 7.4, containing 200 μM $KHSO_5$.

Influence of Primary Sequence, Stereochemistry, and Ionic Strength on Cu(II)· and Ni(II)·ATCUN-Mediated DNA Cleavage. Eight ATCUN metallopeptides with varying primary sequences were tested. In general, the DNA cleavage reactivities of these metallopeptides were observed to increase with an increased number of positively charged Lys residues, as expected based on a simple consideration of their electrostatic attraction

(26) Povirk, L. F.; Wübker, W.; Köhnlein, W.; Hutchinson, F. *Nucleic Acids Res.* **1977**, *4*, 3573−3579.
(27) Freifelder, D. *Biopolymers* **1969**, *7*, 681−693.

Table 3. Comparison of the DNA Linearization (*n*1/*n*2) Activities of Various Cu(II)· and Ni(II)·ATCUN Metallopeptides

peptide	Cu(II) (*n*1/*n*2)	Ni(II) (*n*1/*n*2)
Gly-Gly-His	113	101
Gly-D-Lys-His	61	7
Gly-Lys-His	52	14
D-Lys-Gly-His	33	7
Lys-Gly-His	31	13
Lys-Gly-His-Lys	11	6
Lys-Lys-His	7	2
D-Lys-D-Lys-His	2	5

to DNA (Table 1). The dependence on the presence of Lys residues showed M(II)·Gly-Gly-His to be the weakest DNA cleavage reagent, while the singly substituted systems displayed an increased relative activity and the doubly substituted systems exhibited a further increase in activity (Tables 1 and 2). Interestingly, while the k_2 rate constants for Ni(II)·Lys-Gly-His-Lys, Ni(II)·Lys-Lys-His, and Ni(II)·D-Lys-D-Lys-His were observed to be comparable (Table 1), those for Cu(II)·Lys-Lys-His were always found to be slightly higher, and the linearization efficiency slightly greater (Table 3), than the rates observed for Cu(II)·Lys-Gly-His-Lys. Thus, simple inclusion of an increased number of positive charges does not entirely account for the observed influence of Lys on DNA cleavage rates and linearization propensities.

In comparing the impact of Lys positioning on Cu−metallopeptide reactivity, it appears that a Lys residue in the first position has an overall greater impact on cleavage efficiency than placing this same residue in the second position. Further, in each of these two particular positions, a D-amino acid component appeared to lead to greater reactivity (Table 1). The above findings culminate in the DNA cleavage activity displayed by Cu(II)·D-Lys-D-Lys-His, the metallopeptide with the greatest reactivity among all 10 metallopeptides examined. Thus, these observations indicate that Lys exhibits an influence on DNA cleavage reactivity that is not only altered by its simple positioning in the sequence of the peptide−ligand, but also is influenced by its stereochemistry and/or stereochemical orientation relative to the core metallopeptide equatorial plane.

The ionic strength dependence of activity was also evaluated for both Cu− and Ni−metallopeptide complexes (Supporting Information). With the former, there is a relatively shallow dependence of activity on salt concentration up to 40 mM NaCl. Subsequently, the activity drops off markedly with increasing salt concentration. In contrast, the Ni(II)−ATCUN catalysts demonstrate a more uniform loss of activity with increasing salt concentration, as expected for catalysts that bind principally through an electrostatic mechanism. Free Cu(II) displayed little change in activity except for the highest salt concentration (400 mM) at the highest Cu concentration (10 μM) used, where a modest loss of activity was observed.

Linearization of DNA by Cu(II)· and Ni(II)·ATCUN Metallopeptides. All metallopeptides studied were observed to produce a well-defined electrophoresis band for linear DNA following limited reaction with a supercoiled Form I DNA substrate (Figures 1 and 2); a linear Form III control DNA was prepared and examined in parallel for verification of the presence of this product by digesting plasmid DNA with either *Eco*RI or *Bam*HI restriction endonuclease. To determine the relative linearization capacity of these M(II)−peptide complexes, a standard statistical test was applied.[26,27] This test assumes a Poisson distribution of strand cuts with calculation of the average number of double-strand DNA breaks per molecule, *n*2, from the fraction of linear DNA following strand scission. The total average number of single-strand and double-strand DNA breaks (*n*1 + *n*2) was calculated from the fraction of uncleaved supercoiled DNA.

Table 4. Influence of Lys Positioning and Stereochemistry on the Redox Activities and DNA Cleavage Reactivities of Cu(II)· and Ni(II)·ATCUN Metallopeptides[a]

peptide	ΔE° ($M^{3+/2+}$) (mV) relative to M(III/II)·Gly-Gly-His	D-Lys
Cu(II)·Gly-Lys-His	−11 (k_2 = 46)	−36 (k_2 = 57)
Cu(II)·Lys-Gly-His	−17 (k_2 = 67)	−35 (k_2 = 77)
Cu(II)·Lys-Lys-His	−51 (k_2 = 116)	−75 (k_2 = 200)
Cu(II)·Lys-Gly-His-Lys	−19 (k_2 = 109)	
Ni(II)·Gly-Lys-His	+10 (k_2 =19)	+70 (k_2 = 23)
Ni(II)·Lys-Gly-His	+10 (k_2 = 21)	−20 (k_2 = 26)
Ni(II)·Lys-Lys-His	−10 (k_2 = 35)	−40 (k_2 = 34)
Ni(II)·Lys-Gly-His-Lys	−20 (k_2 = 34)	

[a] Data obtained at pH 7.4 by SWV in phosphate buffer, $[HPO_4]_t^- = 25$ mM, pH 7.4, and 0.1 M KCl. Potentials are quoted as the potential difference relative to the Cu(III/II)·Gly-Gly-His and Ni(III/II)·Gly-Gly-His potentials (obtained relative to NHE) as appropriate. All peptides are amidated on the C-terminus. Negative values indicate a lowering of the potential (less positive) relative to amidated Cu(III/ II)·Gly-Gly-His and Ni(III/II)·Gly-Gly-His, respectively. Values in parentheses are the second-order rate constants (M^{-1} s^{-1}) obtained for the DNA cleavage reactions under oxidative conditions in the presence of ascorbate/O_2. Lys-Gly-His-Lys containing D-Lys was not studied.

The Freifelder−Trumbo relationship indicates that more than 100 single-strand DNA breaks are required to obtain one double-strand DNA break under completely random conditions; thus, the smaller the *n*1/*n*2 value, the higher the linearization activity of an agent in question. In our experiments, the ratios of *n*1/*n*2 for most of the metallopeptide complexes tested (Table 3) were ≪100, and the double-substituted Lys-Lys-His systems yielded values of *n*1/*n*2 in the range 2−7. This observation suggests that ATCUN metallopeptides utilize a nonrandom cleavage path to efficiently form linear DNA. Overall, the general trend in these results parallels the DNA nicking activities reported in Table 1: M(II)·Gly-Gly-His is the least active toward DNA linearization (*n*1/*n*2 > 100) while an increasing number of Lys substitutions leads to an increased linearization propensity; for monosubstituted metallopeptides, Lys in the first position is more active than in the second peptide position (i.e., Cu(II)·Lys-Lys-His > Cu(II)·Lys-Gly-His > Cu(II)·Gly-Lys-His). However, in contrast to the general trend observed in DNA nicking, where D-Lys substitutions appeared to impart increased overall DNA cleavage activity in comparison to their L-Lys isomeric analogues, L/D-Lys diastereoisomeric pairs were found to be similarly active toward DNA linearization.

Influence of Lys Position and Stereochemistry on the Reduction Potentials for Cu(II)· and Ni(II)·ATCUN Metallopeptides. The electrode potential values (vs NHE) for all metallopeptide $Cu^{3+/2+}$ and $Ni^{3+/2+}$ redox couples, relative to those of the corresponding Gly-Gly-His metallopeptides, are listed in Table 4. These values were determined by SWV methods, while the peak separation data (ΔE) were obtained by CV (Supporting Information). These data indicate that C-terminal amidation (vs the presence of a free carboxylate in Gly-Gly-His) increased the electrode potential for formation of Cu(III/II)·Gly-Gly-His (by ∼34 mV), as well as for Ni(III/II)·

Gly-Gly-His (~80 mV) (Supporting Information). In comparison, with the tetrapeptide Lys-Gly-His-Lys, a significant increase in electrode potentials upon amidation of the more remote C-terminus was not observed in either Cu(III)·Lys-Gly-His-Lys (~0.9 mV) or Ni(III)·Lys-Gly-His-Lys (~20 mV).

Further, in the formation of Cu(III)·metallopeptide complexes with Gly-Gly-His, Gly-Lys-His, Lys-Gly-His, Lys-Lys-His, and Lys-Gly-His-Lys (all residues in the L-configuration and with amidated C-termini), the presence of a Lys residue was observed to lower the reduction potential for the $Cu^{3+/2+}$ couple, with two Lys substitutions leading to an even further reduction in this potential. This result is consistent with prior reports[28−30] of the influence of σ-donor groups on the stabilization of the Cu^{3+} state (Table 4). Relative to Gly-Gly-His, Cu^{3+} formation is facilitated in all other peptides containing a Lys residue (Table 4), and a decrease of the positive electrode potential value was indicated by the negative sign.

In comparison to the influence of Lys substitution on the Cu redox couple, the Ni-containing metallopeptides behaved differently. The Ni complexes were relatively insensitive to the σ-donor and electrostatic influences of Lys substitution, but did show greater variation following substitution of L-Lys with D-Lys. Apparently, in the case of the Ni complexes the potentials are more sensitive to the steric consequences of side-chain configuration on the electronic structure at the metal center.

The influence of NaCl on the electrode potentials of a metallopeptide complex was also systematically studied using Cu(II)·Lys-Lys-His and Ni(II)·Lys-Lys-His as examples at four different NaCl concentrations (4, 40, 150, and 400 mM); in each case the potential showed little change with increasing ionic strength.

Discussion

Influence of Amino Acid Sequence and Configuration on DNA Cleavage Reactivity. Consistent with observations discussed in our prior publications,[15a,c] the results of kinetic studies (Table 1) highlight three major factors that influence the DNA cleavage efficiency of a Lys-substituted ATCUN metallopeptide: (1) overall peptide charge, (2) Lys position within the peptide−ligand, and (3) stereochemical orientation. These factors appear to be most applicable to the Cu metallopeptides where, as noted, the cleavage reactivities of the complexes were found to improve with an increased number of positively charged Lys residues. This can be accounted for simply based on an increased electrostatic interaction between the metallopeptide and the DNA. However, an increased electrostatic interaction appears to be only one aspect of the story, since Cu^{2+} derivatives of Gly-Lys-His, Gly-D-Lys-His, Lys-Gly-His, and D-Lys-Gly-His, containing the same number of net positive charges, generally exhibit a higher reactivity when Lys is present at the first position; moreover, Cu metallopeptide complexes containing a D-Lys residue always appear to favor the cleavage reaction relative to those with an L-Lys in the same position (Table 1). Thus, in comparison to all the metallopeptides examined, Cu(II)·D-Lys-D-Lys-His was observed to be the most active toward DNA cleavage with ascorbate or $KHSO_5$ as a co-reactant. As noted elsewhere, the trends displayed by the corresponding nickel complexes (Table 1) occasionally differ from the patterns defined by the Cu metallopeptides, a topic that will be more fully discussed later.

The above observations can be rationalized, in part, through the results of previous NMR and modeling studies.[21,22,24] These studies have indicated that the first amino acid residue of a Cu(II)· or Ni(II)·ATCUN metallopeptide is directed into the minor groove of DNA, while the second amino acid is directed away from the minor groove. Therefore, the first amino acid residue appears to influence DNA recognition and cleavage efficiency in a more pronounced fashion than the amino acid at the second position. Prior structural studies[21,22] also suggest that changing Lys from the L- to the D-configuration in the first peptide position sterically alters the way the metallopeptide complex can approach the DNA minor groove and also the resulting stability of the interaction between the metallopeptide and the DNA. L-Lys generates a metallopeptide that is sterically complementary to the DNA minor groove leading to increased relative site selectivity, while D-Lys sterically prevents a full, stable insertion leading to less site selectivity. In comparison, Lys in the second peptide position, while directed away from the minor groove, leads to L- and D-Lys-substituted metallopeptides that are relatively "thicker" vs "thinner" with regards to their equatorial planes, respectively, allowing those with D-Lys residues to fit more readily into the minor groove and leading to increased cleavage efficiency. While speculative, it is suggested that such structural differences most likely influence the DNA cleavage reaction through a more effective positioning of the reactive metal center relative to a particular scissile bond, perhaps in conjunction with influencing the approach of the metallopeptide "catalyst" to the minor groove. However, as explored herein, there appear to be additional intrinsic properties of each metallopeptide and its diastereoisomers that further complement these structural influences on DNA cleavage activity, such as the redox properties of the metal center.

Comparison of Reduction Potentials and Their Influence on Reactivity. The cyclic voltammograms for the Cu−ATCUN complexes (Supporting Information) show quasi-reversible one-electron redox processes for the $Cu^{3+/2+}$ redox couple and relatively large cathodic and anodic peak potential separations. The Ni−peptides also show quasi-reversible redox processes for the $Ni^{3+/2+}$ redox couple for some of the complexes; complex decomposition was too rapid with Gly-Gly-His and Gly-Lys-His peptides to determine their reversibility, which is further supported by the loss of symmetry obtained in their SWV plots.

With regard to the positional scanning of the Lys residue in the ATCUN motif, it was observed that, relative to Gly-Gly-His, Lys as the first residue tends to stabilize the Cu^{3+} state to a greater extent than if present as the second residue (~17 and 19 mV stabilization in Lys-Gly-His and Lys-Gly-His-Lys, respectively, relative to the ~11 mV stabilization observed for Gly-Lys-His). In the case of the Lys-Lys-His peptide, Cu^{3+}−peptide formation was found to be most facilitated as indicated by its electrode potential (1.018 V, Supporting Information); the impact of two Lys residues appears to be synergistically additive (~50 mV lower relative to Gly-Gly-His, Table 4).

In contrast to the above and in spite of the similarity in overall charge, a comparison of the electrode potentials for Cu(II)·Lys-Lys-His and Cu(II)·Lys-Gly-His-Lys shows considerable variation in their ability to stabilize the Cu^{3+} state. In the case of

(28) Bossu, F. P.; Margerum, D. W. *Inorg. Chem.* **1977**, *16*, 1210−1214.
(29) Bossu, F. P.; Chellappa, K. L.; Margerum, D. W. *J. Am. Chem. Soc.* **1977**, *99*, 2195−2203.
(30) Margerum, D. W.; Owens, G. D. *Met. Ions Biol. Syst.* **1981**, *12*, 75−132.

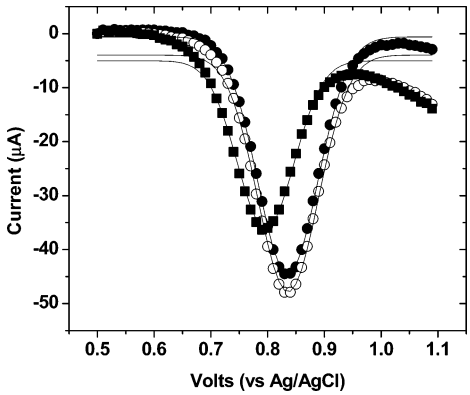

Figure 4. Representative SWV for selected amidated Cu−peptides (● Cu(II)·Gly-D-Lys-His; ○ Cu(II)·D-Lys-Gly-His; ■ Cu(II)·D-Lys-D-Lys-His). Data obtained with 1 mM Cu−peptide (in the presence of 1.1 equiv of peptide, relative to Cu^{2+}) in phosphate buffer, $[HPO_4]_t^- = 25$ mM, pH 7.4, $\mu = 0.1$ M KCl. $E_s = 10$ mV, $E_{sw} = 25$ mV, $f = 100$ Hz, $I/E = -4$. Solid lines are the best Gaussian fits.

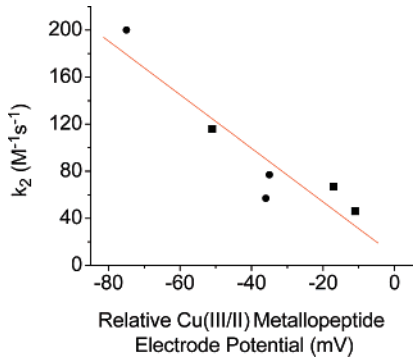

Figure 5. Plot of $Cu^{3+/2+}$ electrode potentials [mV, relative to Cu(II)·Gly-Gly-His] for amidated metallopeptide complexes versus observed second-order rate constant (k_2) for the DNA cleavage reaction. (■) L-Configuration peptides. (●) D-Configuration peptides. Data are taken for the copper tripeptides listed in Table 4 with L- and D-Lys (namely, Cu·Gly-Lys-His, Cu·Lys-Gly-His, and Cu·Lys-Lys-His).

Cu(II)·Lys-Gly-His-Lys, the backbone amide of the fourth Lys residue does not directly coordinate to Cu^{2+} and does not appear to influence the $Cu^{3+/2+}$ reduction potential to the extent that is observed for the Lys-Lys-His complex. Consequently, the stabilization effect appears to reflect only the donor capacity and the spatial orientation of the Lys residues directly connected to the metal coordinating groups, rather than electrostatic contributions. Nevertheless, the net positive charge on each complex would be expected to influence their DNA interactions, as discussed in the previous section. In addition to the σ-donor influence of Lys residues, a change in Lys stereochemistry from L to D was observed to result in enhanced Cu^{3+} stabilization (~35 mV stabilization per Lys residue with respect to Gly-Gly-His) and is additive with respect to the number of Lys residues present (Table 4, Figure 4).

As likely influenced by the above, the DNA cleavage chemistry mediated by M(II)·ATCUN metallopeptides appears to proceed through metal-associated reactive oxygen species that are presumably generated by Fenton-type chemistry under reductive conditions. While we have previously suggested the possibility of peroxide-bridged binuclear copper intermediates en route to ROS formation,[15a] there is currently insufficient data to distinguish a binuclear from a mononuclear pathway. Nevertheless, while reaction via a $Cu^{2+/+}$ couple is normally expected from prototypical Cu^{2+} redox chemistry under these conditions, the redox chemistry of Cu(II)·ATCUN complexes is generally recognized to involve the $Cu^{3+/2+}$ redox couple.[31−33] Thus, to evaluate the influence of redox chemistry on the observed DNA cleavage reactions, the electrode potentials for $Cu^{3+/2+}$ redox couples in complexes containing Gly-Gly-His, Gly-Lys-His, Lys-Gly-His, Lys-Lys-His, and Lys-Gly-His-Lys peptides were correlated with the second-order rate constants (k_2, M^{-1} s^{-1}) obtained for the DNA cleavage reactions containing the respective metal−ATCUN complex (using ascorbate as a co-reactant). The working hypothesis for such a correlation was drawn from the observed trend, which indicated that the presence of a donor group on the α-carbon atom of the ATCUN amino acid residues lowers the $Cu^{3+/2+}$ electrode potential, stabilizing the higher oxidation state. Accordingly, if the higher valent metal species is involved in the DNA cleavage process, its enhanced stabilization should increase the rate of the DNA cleavage reaction. The correlation of electrode potential vs the observed rate constant for the DNA cleavage reaction (Figure 5) indeed supports the hypothesis for the Cu-based system, and each added Lys residue (L-configuration) effectively stabilized the Cu^{3+} state compared to the Gly-Gly-His peptide. However, the linear relationship between rate enhancement for DNA cleavage and addition of Lys residues (effectively lowering the $Cu^{3+/2+}$ potential that is governed by the position of the Lys residue (L form) on the ATCUN motif) breaks down as the stereochemistry of the Lys residue is changed from L to D form (Table 4). Instead, an additive influence of the number of Lys residues (D-form) is seen (Figure 5). Thus, along with the increased stabilization of the Cu^{3+} state that is induced by Lys, the specific orientation of Lys residues, and their impact on the interaction of a metallopeptide with the DNA minor groove, as discussed earlier, both appear to act as important factors governing DNA cleavage efficiency.

The Ni^{2+}−peptides follow a trend similar to that displayed by Cu^{2+}−peptides, but only to a limited extent. An increase in the electrode potential is observed upon amidation of the C-terminal carboxylate (~80 mV for Gly-Gly-His and ~20 mV in Lys-Gly-His-Lys) in tri- and tetrapeptides (Supporting Information); however, the incorporation of a single Lys residue does not contribute toward lowering of the $Ni^{3+/2+}$ electrode potential (with respect to Gly-Gly-His). In fact, it contributes toward an increase in electrode potential to the extent of ~10 mV (Table 4), a trend that is similar to previous reports where highly branched substituents have been shown to destabilize the Ni^{3+}−peptide complexes because of the unfavorable interaction with the axial solvent coordination.[28,29,31] The insensitivity of the $Ni^{3+/2+}$ electrode potential toward a change in the nature of a bound ligand has been observed previously also with less bulky ligands. On the other hand, the incorporation of two Lys residues (as in Lys-Lys-His, Table 4) effectively stabilizes the Ni^{3+} state in the Ni(III)·Lys-Lys-His complex relative to the unsubstituted Gly-Gly-His peptide. The stabilization effect observed for the Ni(III)·Lys-Lys-His complex is further enhanced upon a change in Lys stereochemistry from L to D (Table 4) and is consistent with that observed in the corre-

(31) Murray, C. K.; Margerum, D. W. *Inorg. Chem.* **1982**, *21*, 3501−3506.
(32) McDonald, M. R.; Scheper, W. M.; Lee, H. D.; Margerum, D. W. *Inorg. Chem.* **1995**, *34*, 229−237.
(33) McDonald, M. R.; Fredericks, F. C.; Margerum, D. W. *Inorg. Chem.* **1997**, *36*, 3119−3124.

sponding Cu analogue, but to a significantly lower extent. The deviation from the additive trend observed for Lys residues in Ni−peptide complexes as compared to that in Cu−peptides could, therefore, reflect the geometric influence of electronic configuration for the d^7 system in Ni^{3+}, relative to the d^8 configuration in the case of Cu^{3+}. Consequently, the variations from general trends would reflect the large gain in LFSE accompanying the transition from d^9 (Cu^{2+}) to d^8 (Cu^{3+}), relative to the smaller gain in LFSE for the transition from d^8 (Ni^{2+}) to d^7 (Ni^{3+}).[28,29]

An important distinction between the Cu(II)· and Ni(II)· ATCUN complexes is worth noting here. While the Cu(II)· ATCUN complexes are invariably found to demonstrate superior DNA cleavage ability with ascorbate as a co-reactant, the relative activities of the Cu vs Ni metallopeptides are more comparable when oxone is used as a co-reactant (k_2, Table 2). This presumably reflects the relative ease of formation of reactive oxygen species by Cu(II)·ATCUN complexes with the milder reducing agent ascorbate versus the harsher oxone system. Other experimental studies (unpublished data as well as a comparison of data in Tables 1 and 2) suggest that the Ni derivatives are less capable of efficiently mediating formation of peroxide intermediates from ascorbate/dioxygen, demonstrating enhanced activity only when the peroxide is provided as a preformed activated species.

Finally, differences in the reaction mechanisms and efficiencies of Cu(II)·ATCUN vs Ni(II)·ATCUN metallopeptides may result also from subtle variations in the orientation and positioning of their respective metal-associated reactive oxygen species proximally to distinct DNA scissile bonds. There is insufficient detailed characterization of reaction products from the use of Cu(II)· and Ni(II)·ATCUN derivatives to define these differences in great detail. However, for example, we reported earlier[20] that the ratios of alkaline labile to propenal product formation resulting from C4′−H abstraction differ for Ni(II)·Lys-Gly-His and Ni(II)·Gly-Gly-His; Ni(II)·Lys-Gly-His promotes the formation of an increased relative amount of the two electron abstraction product, nucleobase propenal. In light of the results presented herein, this observation suggests inherent mechanistic differences upon Lys substitution.

Influence of Ionic Strength on Binding, Reduction Potentials, and Reactivity. While the reduction potentials for both Cu and Ni metallopeptides showed little change over the range of ionic strength studied, both demonstrated a decrease in complex-promoted cleavage activity with increasing salt concentration. In the case of Ni derivatives, the change was rather straightforward, where the cleavage reactivity was observed to decrease uniformly as a function of increasing salt concentration (Supporting Information). However, with Cu metallopeptides a lag phase was observed up to ~40 mM NaCl, suggesting the possibility of direct Cu coordination as an additional binding component (notably, control experiments with free Cu^{2+} also displayed minimal ionic strength dependence). The distinct behaviors of Cu and Ni complexes again support the notion that underlying metal-centered differences influence their respective DNA cleavage reactivities.

Factors Promoting DNA Linearization. The general trend observed for M(II)·ATCUN-promoted linearization of supercoiled DNA is similar to the trend exhibited in the overall DNA cleavage activity of these complexes (Tables 1 and 3). Most of the $n1/n2$ values determined were significantly smaller than 100, indicating a nonrandom cleavage pathway leading to DNA linearization. DNA linearization requires two nicks, one on each of the complementary DNA strands within 10 base pairs of each other. As such, the observation of nonrandom linearization of DNA requires that a metallopeptide associate with a localized region of a DNA substrate with sufficient residence time to allow for its appropriate positioning and repositioning to mediate cleavage of both DNA strands. Clearly the sequence, amino acid configuration, and redox factors discussed earlier in our analysis of reactivity, and in prior published work,[15a] are also dominant in promoting linearization of DNA. This is not unexpected inasmuch as linearization will be promoted by rapid cleavage of both strands during the residency time for an association event, which in turn should correlate with the intrinsic reactivity of the catalytic complexes.

Correlation of DNA Cleavage Reactivities to the Redox Properties of Cu(II)· and Ni(II)·ATCUN Metallopeptides. These experiments demonstrate the dependence of metal−ATCUN-promoted DNA cleavage chemistry on peptide sequence (specifically the number and position of positively charged Lys residues), amino acid configuration, as well as the $M^{3+/2+}$ reduction potential of the ATCUN-bound metal center. Variation of the identity (Lys vs Gly) and/or configuration (for Lys) of the first amino acid position has the greatest impact on selectivity[21,22] as well as reactivity, while increasing positive charge density results in a general increase in reactivity. For Cu complexes, the D-Lys-substituted isomers show potentials that are more negative (the Cu^{3+} state is more stable) relative to the corresponding L-Lys isomers. Again the impact is most noticeable for changes at the first amino acid position. Such changes in potential reflect stereochemical tuning of the σ-donor character of Lys side chains. While Cu and Ni peptide complexes show similar trends in reactivity with an increasing number of Lys residues, the detailed trends are distinct with respect to the position and configuration of the Lys residues. In stark contrast to the Cu derivatives, there is no clear dependence of reactivity with reduction potential in the case of the Ni peptides. Such deviations underscore the differences in the electronic (and consequently geometric) structures of the $Cu^{3+/2+}$ vs the $Ni^{3+/2+}$ complexes.

For both Cu(II)· and Ni(II)·ATCUN-catalyzed DNA cleavage chemistry, reactivity appears to be mediated by metal-associated reactive oxygen species that are formed by way of the $M^{3+/2+}$ redox couples. For Cu derivatives, the overall charge, impact of changing configuration, and influence of Cu reduction potentials all influence reactivity in a fairly uniform manner. It is noteworthy that the structure of Cu in both d^8 and d^9 configurations is expected to be similar (square planar). In the case of Ni derivatives, the absence of a clear correlation of reactivity with reduction potential emphasizes the importance of subtle orientation effects in positioning the metal-associated reactive oxygen species for optimum reactivity. Clearly, the Ni derivatives are much more sensitive to such orientational restrictions than the corresponding Cu complexes and may reflect the distinct coordination geometries of the d^7 and d^8 configurations for Ni and the timing of productive cleavage chemistry relative to change in the redox state at the Ni center.

Major differences in reactivity for the Cu and Ni complexes appear to reflect orientational effects, rather than reduction potentials, where the metal-associated ROS is positioned more or less optimally to mediate chemistry at particular scissile bonds on the nucleic acid backbone or nucleobases. This is a viewpoint that is consistent with prior characterization of reaction products.[15] Assuming the catalysts to be capable of forming a metal-associated ROS, it is the position of the ROS relative to scissile bonds that will ultimately dictate relative reactivity and will be influenced by the peptide structural factors discussed herein.

Acknowledgment. We acknowledge the National Institutes of Health for financial support of this work (GM 63740 to J.A.C. and GM 62831 to E.C.L.).

Supporting Information Available: Cyclic voltammograms, a summary of electrode potentials, and salt dependence of DNA cleavage activity. This material is available free of charge via the Internet at http://pubs.acs.org.

JA0705083